

Synthesis, spectroscopy and computational studies of some biologically important hydroxyhaloquinolines and their novel derivatives

Grzegorz Malecki^a, Jacek E. Nycz^{a,*}, Ewa Rych^a, Lukasz Ponikiewski^c, Maria Nowak^b, Joachim Kusz^b, Jerzy Pikies^c

^aInstitute of Chemistry, University of Silesia, ul. Szkolna 9, PL-40006 Katowice, Poland

^bInstitute of Physic, University of Silesia, ul. Uniwersytecka 4, PL-40006 Katowice, Poland

^cDepartment of Inorganic Chemistry, Faculty of Chemistry, Gdańsk University of Technology, 11/12G. Narutowicz St., PL-80233 Gdańsk, Poland

ARTICLE INFO

Article history:

Received 15 December 2009

Received in revised form 20 January 2010

Accepted 20 January 2010

Available online 1 February 2010

Keywords:

Quinoline

Haloquinoline

DFT

Phosphorylation

HIV

Anti-malarial

ABSTRACT

A series crystalline compounds of methyl and phosphinyl derivatives of 2-methylquinolin-8-ol (**1a**) and related 5,7-dichloro-2-methylquinolin-8-ol (**1b**) were quantitatively prepared and characterized by microanalysis, IR, UV–vis and multinuclear NMR spectroscopy. Five of them have been characterized by single crystal X-ray diffraction method. The known compounds, 8-methoxy-2-methylquinoline (**2a**) and 8-methoxyquinoline (**2d**), were synthesised by a new route. NMR solution spectra at ambient temperature, showed readily diagnostic H-1 and C-13 signals from methyl groups. The geometries of the studied compounds were optimized in singlet states using the density functional theory (DFT) method with B3LYP functional. In general, the predicted bond lengths and angles are in a good agreement with the values based on the X-ray crystal structure data. Electronic spectra were calculated by TDDFT method.

Crown Copyright © 2010 Published by Elsevier B.V. All rights reserved.

1. Introduction

Compounds containing quinoline structure have been extensively studied and widely used for the design and development of large variety of medical drugs, especially since the discovery of Cinchona alkaloids as antimalarial agents. In particular, chloroquine, quinine and amodiaquine have proved to be among the most effective anti-malarial drugs [1–3]. Systematic modification of quinine led to diverse quinoline anti-malarial drugs with diverse substitutions around the quinoline rings. One of the first drugs to be prepared was the potent and inexpensive chloroquine [4], which is a 7-chloroquinoline with an amino substituent in position 4.

2-Methylquinolin-8-ol (**1a**) and related 5,7-dichloro-2-methylquinolin-8-ol (**1b**) have received significant attention, as evident from ca. 600 papers on this topic published only in 1990–2009 [Scifinder]. Surprisingly, there are no single crystal X-ray structures reported so far. The persistent interest is not only from the fact that these compounds have attracted special attention due to its strong antibacterial, antifungal, trichomonal and keratoplastic effect [5–9], but also because they are important synthetic intermediates for the preparation of a variety of biologically active compounds [9].

They are a family of polar ligands with peculiar properties since they may change either their hydrogen-bond donating or accepting sites through the protonation/deprotonation processes [10].

Herein, we report full spectroscopic characterization and X-ray analysis of single crystal structures for five hydroxy-2-methylquinolines derivatives.

2. Experimental

2.1. General

All experiments were carried out in an atmosphere of dry argon. Solvents were dried by usual methods (benzene and THF over benzophenone ketyl, CHCl₃ and CH₂Cl₂ over P₂O₅, hexane over sodium–potassium alloy), distilled and degassed. Chromatography was carried out on Silica Gel 60 (0.15–0.30 mm) Machery Nagel. Melting points are uncorrected. NMR spectra were obtained with Bruker Avance 400 operating at 400.13 MHz (¹H), 100.5 MHz (¹³C) and 161.9 MHz (³¹P) at 30 °C; chemical shifts referenced to ext. TMS (¹H, ¹³C), 85% H₃PO₄ (³¹P); coupling constants are given in Hz. IR spectra were recorded on a Nicolet Magna 560 spectrophotometer in the spectral range 4000–400 cm⁻¹ with the samples in the form of KBr pellets. Electronic spectra were measured on a spectrophotometer Lab Alliance UV–vis 8500 in the range 1000–180 nm in CH₂Cl₂ solution. Mass spectra were obtained with a

* Corresponding author. Tel.: +48 323591206; fax: +48 322599978.

E-mail address: jnycz@us.edu.pl (J.E. Nycz).

Finnigan MAT 95 (Brema, Germany) in EI mode and, where necessary, FAB technique was applied. Elemental analysis: Perkin-Elmer 2400CHSN/O Analyser. Compounds 5,7-dibromo-2-methylquinolin-8-ol (**1c**), **1d** were purchased from Sigma–Aldrich, and were used without further purification.

2.2. Crystal structure determination and refinement

Data for compounds **1a** and **3a** were collected on a KM4 diffractometer using Sapphire-2 CCD detector, for **1b** and **2a** the data were obtained during the measurement performed on a KM4 diffractometer equipped with Sapphire-3 CCD detector and for **3b** was collected on a STOE IPDS 2-circle diffractometer. For all measurements graphite-monochromated Mo-K α radiation was used. The crystals were cooled down by a cold dry nitrogen gas stream (Oxford Cryosystems equipment). The temperature stability was ± 1 K.

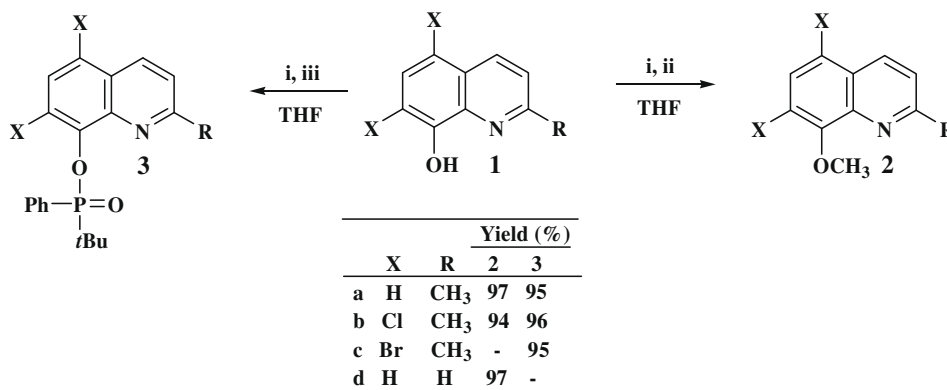
The structures **1a**, **3a** and **3b** were solved by direct methods and refined by full-matrix least-squares on F2 (all data) using the SHELXTL program package [11]. The structures **1b** and **2a** were first solved using the direct method with SHELXS-97 software [12] and then the solutions were refined with SHELXL-97 [12]. All non-hydrogen atoms were refined anisotropically. Atomic scattering factors had values incorporated in the computer programs. All H atoms bound to C atoms were refined using a riding model with C–H distances of 0.95 Å or 0.98 Å and Uiso(H) values of 1.2 Ueq(C) or 1.5 Ueq(C), respectively. H atoms, which took part in hydrogen bond, were permitted to ride at the positions deduced from the difference maps with Uiso(H) equal to 1.2 Ueq(C) or 1.5 Ueq(O).

CCDC-739462 (**1a**), CCDC-736932 (**1b**), CCDC-746254 and CCDC-746255 (**2a**), CCDC-739463 (**3a**), CCDC-739464 (**3b**) contain the supplementary crystallographic data (excluding structure factors) for this paper. These data can be obtained free of charge via <http://www.ccdc.cam.ac.uk/conts/retrieving.html> (or from the Cambridge Crystallographic Data Centre, 12, Union Road, Cambridge CB2 1EZ, UK; fax: +44 1223 336033).

2.3. Synthesis

Compounds, **1a** was purchased from Sigma–Aldrich, **1b** was purchased from ICN Polfa Rzeszow S.A. and were used with further purification.

Compound **1a** sublimation and crystallization (PhH); mp = 74 °C; ^1H NMR (CDCl_3) δ = 2.73 (s, 3H, CH_3), 7.19 (dd, J_{HH} = 7.6 Hz, J_{HH} = 1.1 Hz, 1H, H-quinoline), 7.29 (d, J_{HH} = 8.5 Hz, 1H, H-quinoline), 7.29 (d, J_{HH} = 8.2 Hz, 1H, H-quinoline), 7.40 (t, J_{HH} = 7.9 Hz, 1H, H-quinoline), 8.02 (d, J_{HH} = 8.4 Hz, 1H, H-quinoline); $^{13}\text{C}\{^1\text{H}\}$ NMR (CDCl_3) 24.75, 109.87, 117.49, 122.60, 126.53, 126.57, 136.11, 137.51, 151.61, 156.77; UV–vis: 306.0 nm.



Scheme 1. Reagents and conditions: i – Bu^tOK , reflux; ii – CH_3I , r.t.; iii – $\text{Ph}(\text{Bu}^t)\text{P}(\text{O})\text{Cl}$, reflux.

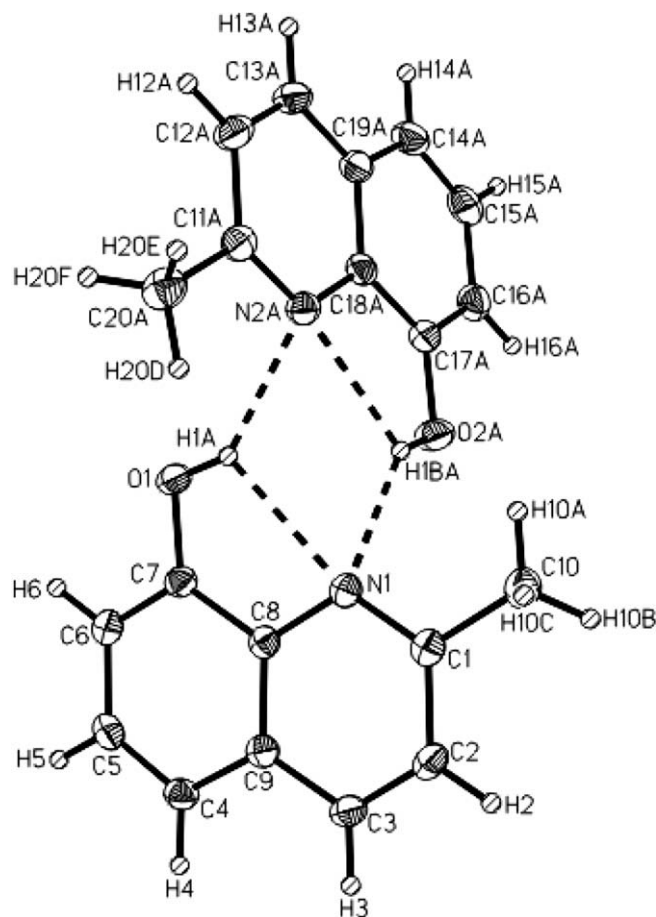


Fig. 1. Molecular structure diagrams of **1a** (the thermal ellipsoids are drawn at the 50% probability level).

Compound **1b** crystallization (PhCH_3); mp = 113–114 °C; ^1H NMR (CDCl_3) δ = 2.74 (s, 3H, CH_3), 7.38 (d, J_{HH} = 8.6 Hz, 1H, H-quinoline), 7.47 (s, 1H, H-quinoline), 8.30 (d, J_{HH} = 8.6 Hz, 1H, H-quinoline); $^{13}\text{C}\{^1\text{H}\}$ NMR (CDCl_3) 24.71, 115.15, 120.59, 123.10, 123.39, 127.17, 133.55, 137.82, 146.98, 158.77; UV–vis: 318.0 nm.

2.4. Synthesis of **2a**, **2b** and **2d**

Into the solution of **1a** or **1b** (5.0 mmol) in THF (25 mL), $t\text{BuOK}$ (0.616 g, 5.5 mmol) was added. The reaction was carried out for 3 h under reflux. Subsequently at r.t., CH_3I (5.0 mmol) was added. The reaction was carried out for 6 h at r.t. Next, CH_2Cl_2 KHSO_4 water

solution was added. The organic phase was dried (MgSO_4), and the solvent was evaporated and the crude product was purified by sublimation, chromatography and crystallization.

8-Methoxy-2-methylquinoline (2a) 0.839 g (4.85 mmol, 97%); mp = 126 °C; bp = 118–119 °C/1.0 mm Hg; ^1H NMR (CDCl_3) δ = 2.77 (s, 3H, CH_3), 4.05 (s, 3H, CH_3), 7.00 (dd, $J_{\text{HH}} = 7.2$ Hz, $J_{\text{HH}} = 1.8$ Hz, 1H, H-quinoline), 7.27 (d, $J_{\text{HH}} = 8.5$ Hz, 1H, H-quinoline), 7.28–7.39 (m, 2H, H-quinoline) 7.98 (d, $J_{\text{HH}} = 8.1$ Hz, 1H, H-quinoline); $^{13}\text{C}\{^1\text{H}\}$ NMR (CDCl_3) 25.70, 55.96, 107.58, 119.38, 122.54, 125.63, 127.55, 136.050, 139.71, 154.82, 158.09; E.A.

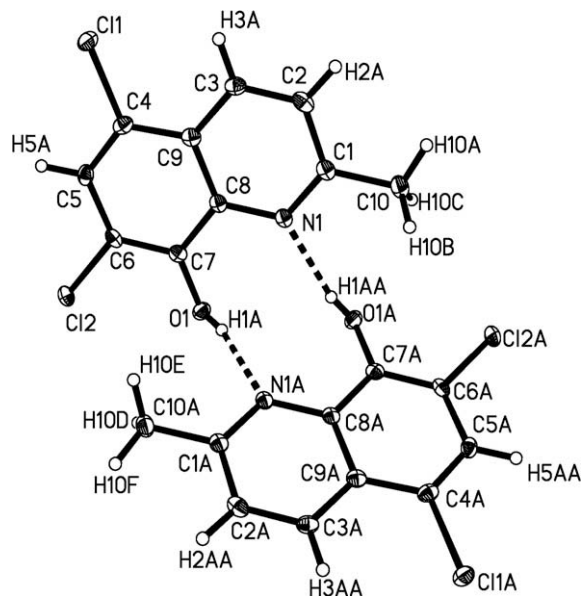


Fig. 2. Molecular structure diagrams of **1b** (the thermal ellipsoids are drawn at the 50% probability level).

Table 1
Selected bond lengths and angles for **1a**.

Bond lengths (Å)				
C7–O1	1.3520(15)	C15–C16	1.4087(19)	
C17–O2	1.3592(15)	N1–C1	1.3211(16)	
C1–C10	1.5007(18)	N1–C8	1.3694(16)	
C11–C20	1.4967(18)	N2–C11	1.3197(16)	
C5–C6	1.4065(18)	N2–C18	1.3711(16)	
Hydrogen-bond geometry (Å, °)				
D–H...A	D–H	H...A	D...A	D–H...A
O1–H1A...N1	0.86(2)	2.330(19)	2.7695(14)	112.2(15)
O1–H1A...N2A	0.86(2)	2.132(19)	2.8261(15)	138.0(16)
O2A–H1BA...N1	0.86(2)	2.160(2)	2.8700(15)	139.1(19)
O2A–H1AB...N2A	0.86(2)	2.330(2)	2.7729(14)	111.7(17)

Table 2
Selected bond lengths and angles for **1b**.

Bond lengths (Å)				
C7–O1	1.348(10)	N1–C1	1.330(12)	
C6–C12	1.734(16)	N1–C8	1.371(19)	
C4–C11	1.752(16)	C6–C7	1.387(19)	
C4–C9	1.418(2)	C4–C5	1.365(12)	
C1–C10	1.507(20)	C6–C5	1.413(13)	
Hydrogen-bond geometry (Å, °)				
D–H...A	D–H	H...A	D...A	D–H...A
O1–H1A...N1A	0.80(2)	1.92(2)	2.6967(13)	165.2(19)°

[Found C, 76.02; H, 6.39; N, 8.13; $\text{C}_{11}\text{H}_{11}\text{NO}$ requires C, 76.28; H, 6.40; N, 8.29%]; UV-vis: 300.0 nm.

5,7-Dichloro-8-methoxy-2-methylquinoline (2b) crystallization (CH_2Cl_2 hexane) 2.148 g (4.7 mmol, 94%); mp = 110 °C; ^1H NMR (CDCl_3) δ = 2.80 (s, 3H, CH_3), 4.17 (s, 3H, CH_3), 7.38 (d, $J_{\text{HH}} = 8.7$ Hz, 1H, H-quinoline), 7.56 (s, 1H, H-quinoline), 8.38 (d, $J_{\text{HH}} = 8.7$ Hz, 1H, H-quinoline); $^{13}\text{C}\{^1\text{H}\}$ NMR (CDCl_3) 25.55, 62.27, 122.89, 124.59, 126.09, 126.55, 126.80, 133.30, 143.29, 151.05, 160.14; E.A. [Found C, 54.53; H, 3.58; N, 5.49; $\text{C}_{11}\text{H}_9\text{Cl}_2\text{NO}$ requires C, 54.57; H, 3.75; N, 5.79%]; UV-vis: 326.4, 300.8 nm.

8-Methoxyquinoline (2d) 0.771 g (4.8 mmol, 97%); mp = 48 °C; bp = 175–176 °C/17 mm Hg; ^1H NMR (CDCl_3) δ = 4.06 (s, 3H, CH_3), 7.02 (dd, $J_{\text{HH}} = 7.5$ Hz, $J_{\text{HH}} = 1.3$ Hz, 1H, H-quinoline), 7.33–7.46 (m, 3H, H-quinoline), 8.08 (dd, $J_{\text{HH}} = 8.3$ Hz, $J_{\text{HH}} = 1.7$ Hz, 1H, H-quinoline), 8.89 (dd, $J_{\text{HH}} = 4.2$ Hz, $J_{\text{HH}} = 1.73$ Hz, 1H, H-quinoline); $^{13}\text{C}\{^1\text{H}\}$ NMR (CDCl_3) 55.93, 107.51, 119.51, 121.63, 126.66, 129.34, 135.80, 140.23, 149.22, 155.42; E.A. [Found C, 74.93; H, 5.65; N, 8.80; $\text{C}_{10}\text{H}_9\text{NO}$ requires C, 75.45; H, 5.70; N, 8.80%]; UV-vis: 303.2 nm.

2.5. Synthesis of 3a–c

$\text{Ph}(\text{Bu}^t\text{P})(\text{O})\text{Cl}$ (5.0 mmol) was added to the suspension of NaH (0.133 g, 5.5 mmol) in THF (25 mL). Subsequently, **1a** (or **1b** or **1c**) (5.0 mmol), was added. The reaction was carried out for 24 h under reflux. Next, CH_2Cl_2 KHSO_4 water solution was added. The organic phase was dried (MgSO_4), and the solvent was evaporated

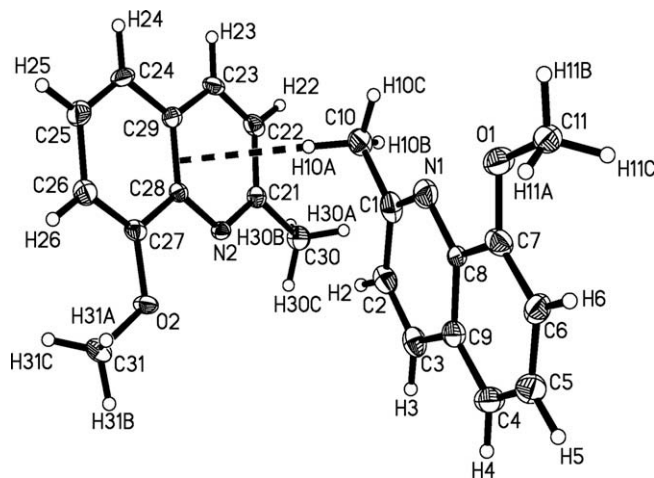


Fig. 3. Molecular structure diagrams of **2a** (the thermal ellipsoids are drawn at the 50% probability level).

Table 3
Selected bond lengths and angles for **2a**. Cg denotes the centroid of the quinoline ring.

Bond lengths (Å)				
C7–O1	1.353(3)	C4–C5	1.367(3)	
O1–C11	1.434(3)	C4–C9	1.403(3)	
C1–C10	1.499(3)	N1–C1	1.302(3)	
C22–C31	1.497(3)	N1–C8	1.367(3)	
C6–C7	1.381(3)	C26–C27	1.414(3)	
C5–C6	1.405(3)			
Bond angles (°)				
C7–O1–C11	116.57(17)	C27–O2–C31	117.26(16)	
Hydrogen-bond geometry (Å, °)				
D–H...A	D–H	H...A	D...A	D–H...A
C11–H11A ... Cg	0.95(2)	2.85(3)	3.757(11)	159.71 (1.93)

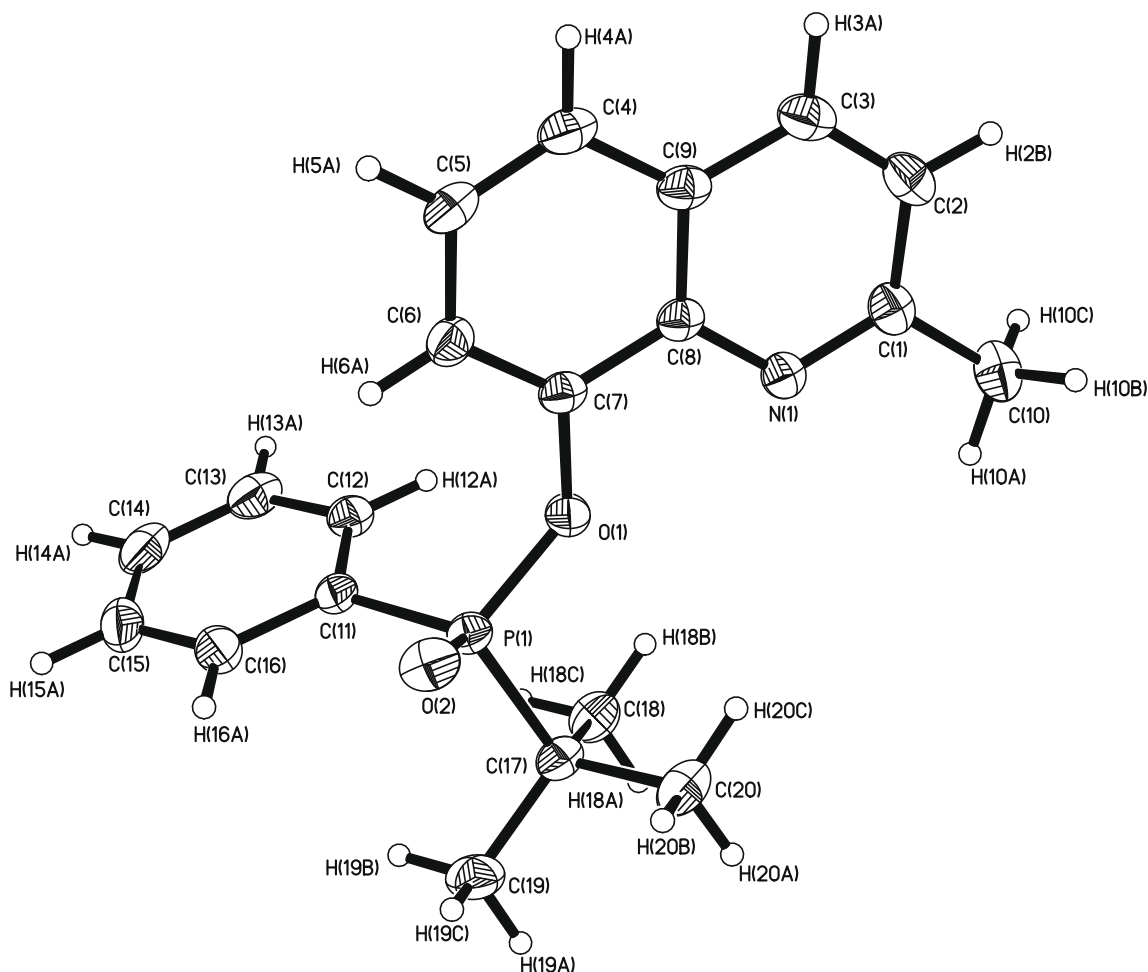


Fig. 4. Molecular structure diagrams of **3a** (the thermal ellipsoids are drawn at the 50% probability level).

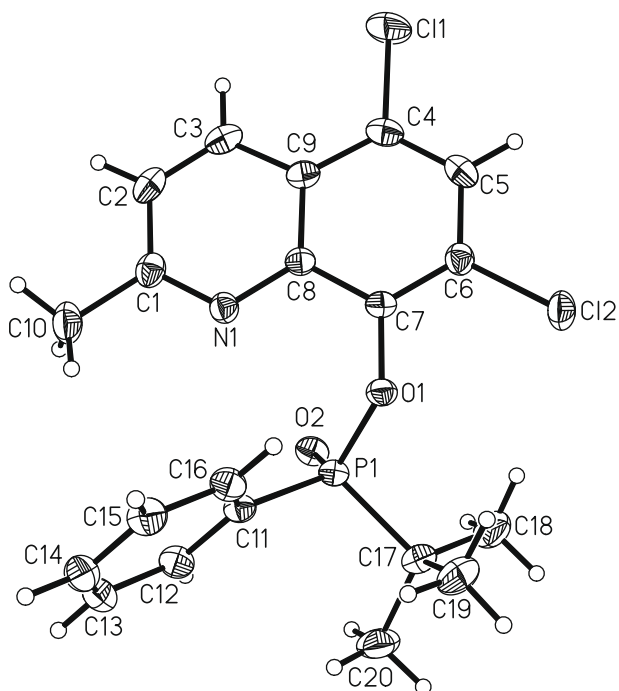


Fig. 5. Molecular structure diagram of **3b** (the thermal ellipsoids are drawn at the 50% probability level).

and the crude product was purified by chromatography and crystallization:

2-Methylquinolin-8-yl tert-butyl(phenyl)phosphinate (3a) crystallization (CH_2Cl_2 : hexane); 1.610 g (4.8 mmol, 95%); mp = 112 °C; ^1H NMR (CDCl_3) δ = 1.36 (d, $^3J_{\text{PH}} = 16.0$ Hz, 9H, Bu^t), 2.71 (s, 3H, CH_3), 7.24 (d, $J_{\text{HH}} = 8.3$ Hz, 1H, aromatic-Q), 7.29 – 7.38 (m, 2H, aromatic), 7.42 (2dd, $J_{\text{HH}} = 1.4$ Hz, $J_{\text{HH}} = 7.6$ Hz, 2H, aromatic-Q), 7.65 (td, $J_{\text{HH}} = 1.4$ Hz, $J_{\text{HH}} = 7.7$ Hz, 1H, aromatic-Q), 7.93 (d, $J_{\text{HH}} = 8.4$ Hz, 1H, aromatic-Q), 8.02–8.05 (m, 2H, aromatic), 8.04 (dd, $J_{\text{HH}} = 1.4$ Hz, $^3J_{\text{P-H}} = 17.4$ Hz, 1H, aromatic); $^{13}\text{C}\{^1\text{H}\}$ NMR (CDCl_3) 24.38, 25.49,

Table 4

Selected bond lengths and angles for **3a**. Symmetry codes: (i) $1 - x, -1/2 + y, 1/2 - z$, (ii) $x, 1.5 - y, -1/2 + z$.

Bond lengths (Å)				
C7–O1	1.3920(2)	C6–C7	1.3680(3)	
P1–O1	1.6042(18)	C4–C9	1.4140(3)	
P1–O2	1.4740(13)	N1–C1	1.3200(2)	
C4–C5	1.3630(4)	N1–C8	1.3680(2)	
C5–C6	1.4090(3)			
Bond angles [°]				
C7–O1–P2	125.79(11)	O1–P1–O2	115.70(7)	
Hydrogen-bond geometry (Å, °)				
D–H...A	D–H	H...A	D...A	D–H...A
C15–H15A...O2 ⁽ⁱ⁾	0.94(2)	2.38(2)	3.180(2)	143.2(19)
C18–H18A...O2 ⁽ⁱⁱ⁾	1.00(3)	2.60(2)	3.419(2)	139.9(18)

33.96 ($J_{CP} = 100$ Hz), 119.50 ($J_{CP} = 4$ Hz), 122.20, 123.27, 125.37 ($J_{CP} = 1$ Hz), 127.66 ($J_{CP} = 18$ Hz), 127.83 ($J_{CP} = 12$ Hz), 129.37, 131.96 ($J_{CP} = 3$ Hz), 133.56 ($J_{CP} = 9$ Hz), 130.72, 140.73 ($J_{CP} = 4$ Hz), 147.23 ($J_{CP} = 10$ Hz), 158.48; $^{31}\text{P}\{^1\text{H}\}$ NMR (CDCl_3) $\delta = 51.54$; EI-MS (m/z , %) 340.3 (6, $[\text{M}]^+$), 282.2 (100, $[\text{M}]-\text{Bu}^t$) $^+$; E.A. [Found C, 70.50; H, 6.57; N, 4.10; $\text{C}_{20}\text{H}_{22}\text{NO}_2\text{P}$ requires C, 70.78; H, 6.53; N, 4.13%]; UV-vis: 319.3, 283.4, 272.9 nm.

5,7-Dichloro-2-methylquinolin-8-yl tert-butyl(phenyl)phosphinate (3b) crystallization (CH_2Cl_2 : hexane); 1.958 g (4.8 mmol, 96%); mp = 205–206 °C; ^1H NMR (CDCl_3) $\delta = 1.37$ (d, $^3J_{\text{PH}} = 16.1$ Hz, 9H, Bu^t), 2.04 (s, 3H, CH_3), 7.19 (d, $J_{\text{HH}} = 8.7$ Hz, 1H, aromatic-Q), 7.47 (dt, $J_{\text{HH}} = 3.6$ Hz, $^3J_{\text{PH}} = 7.4$ Hz, 2H, P-Ph-o), 7.54 (dd, $J_{\text{HH}} = 1.3$ Hz, $^3J_{\text{PH}} = 7.1$ Hz, 1H, P-Ph-p), 7.56 (s, 1H, aromatic-Q), 7.93 (ddd, $J_{\text{PH}} = 10.9$ Hz, $J_{\text{HH}} = 8.2$ Hz, $J_{\text{HH}} = 1.6$ Hz, 2H, P-Ph-m); 8.24 (d, $J_{\text{HH}} = 8.7$ Hz, 1H, aromatic-Q); $^{13}\text{C}\{^1\text{H}\}$ NMR (CDCl_3) 23.59, 24.18, 34.75 ($J_{CP} = 98$ Hz), 123.13, 124.13, 124.46 ($J_{CP} = 5$ Hz), 126.37, 126.63 ($J_{CP} = 1$ Hz), 127.59 ($J_{CP} = 12$ Hz), 130.86, 131.03 ($J_{CP} = 3$ Hz), 132.19 ($J_{CP} = 9$ Hz), 132.41, 132.82, 141.17 ($J_{CP} = 2$ Hz), 143.88 ($J_{CP} = 12$ Hz), 159.44; $^{31}\text{P}\{^1\text{H}\}$ NMR (CDCl_3) $\delta = 53.17$; MS (FAB) (m/z , %) 408 (100%, $[\text{M}]^+$); HRMS: m/z Calcd for $\text{C}_{20}\text{H}_{21}\text{NPO}_2\text{Cl}_2$ ($\text{M} + \text{H}$) $^+$: 408.06886 Found 408.068699; E.A. [Found C, 58.75; H, 5.13; N, 3.43; $\text{C}_{20}\text{H}_{20}\text{Cl}_2\text{NO}_2\text{P}$ requires C, 58.84; H, 4.94; N, 3.43%]; UV-vis: 300.2 nm.

5,7-Dibromo-2-methylquinolin-8-yl tert-butyl(phenyl)phosphinate (3c) crystallization (CHCl_3 : hexane); 2.361 g (4.8 mmol, 95%); mp = 203 °C; ^1H NMR (CDCl_3) $\delta = 1.35$ (d, $^3J_{\text{PH}} = 16.0$ Hz, 9H, Bu^t), 1.99 (s, 3H, CH_3), 7.15 (d, $J_{\text{HH}} = 8.7$ Hz, 1H, aromatic-Q), 7.37–7.54 (m, 3H, aromatic-Q), 7.84–7.92 (m, 3H, aromatic-Q), 8.16 (d, $J_{\text{HH}} = 8.7$ Hz, 1H, aromatic-Q); $^{13}\text{C}\{^1\text{H}\}$ NMR (CDCl_3) 23.30, 24.87, 34.78 ($J_{CP} = 99$ Hz), 113.50, 119.15, 123.65, 125.92, 127.51, 127.71, 130.90, 130.94, 131.93, 132.07, 132.40, 134.95, 159.22; $^{31}\text{P}\{^1\text{H}\}$ NMR (CDCl_3) $\delta = 52.70$; EI-MS (m/z , %) 496.9 (17, $[\text{M}]^+$); E.A. [Found C, 49.44; H, 4.16; N, 2.78; $\text{C}_{20}\text{H}_{20}\text{Br}_2\text{NO}_2\text{P}$ requires C, 48.32; H, 4.05; N, 2.82%]; UV-vis: 300.2 nm.

3. Results and discussion

The reactions of hydroxyhaloquinolines **1a–d** with Bu^tOK were carried out under reflux with a set of identical reaction conditions (Scheme 1). Subsequently electrophiles were added. For CH_3I the

reaction was carried out for 6 h at room temperature. $\text{Ph}(\text{Bu}^t)\text{-P}(\text{O})\text{Cl}$ was found less reactive and required heating because of steric and electronic reasons. All products, **2a**, **2b**, **2d** and **3a–c** were isolated with high yields (94–97%).

The reagents **1a** and **1b** were chosen as model compounds, and were characterised by X-ray crystal structure analysis (Figs. 1 and 2; Tables 1 and 2), which showed the presence of hydrogen-bond

Table 5
Selected bond lengths and angles for **3b**. Symmetry codes: (i) $x, -1/2 - y, 1/2 + z$, (ii) $2 - x, -y, -z$.

Bond lengths (Å)				
C7–O1	1.3762(15)	C5–C6	1.4106(16)	
O1–P1	1.6231(10)	C6–C7	1.378(18)	
P1–O2	1.4745(10)	C4–C9	1.4140(18)	
C4–Cl1	1.7409(14)	N1–C1	1.3194(18)	
C6–Cl2	1.7272(14)	N1–C8	1.3547(17)	
C4–C5	1.3600(9)			
Bond angles (°)				
C7–O1–P1	125.20(7)	O1–P1–O2	114.85(5)	
Hydrogen-bond geometry (Å, °)				
D–H...A	D–H	H...A	D...A	D–H...A
C2–H2...O2 ⁽ⁱ⁾	0.949(18)	2.369(18)	3.2695(17)	158.3(15)
C12–H12A...O2 ⁽ⁱⁱ⁾	0.929(18)	2.348(18)	3.266(2)	169.5(15)

Table 6
The ^1H and ^{13}C chemical shifts of methyl group in DMSO-d_6 .

	1a	1b	2a	2b	3a	3b	3c
^1H	2.73	2.74	2.77	2.80	2.71	2.04	1.99
^{13}C	24.75	24.71	25.70	25.55	25.49	24.18	24.87

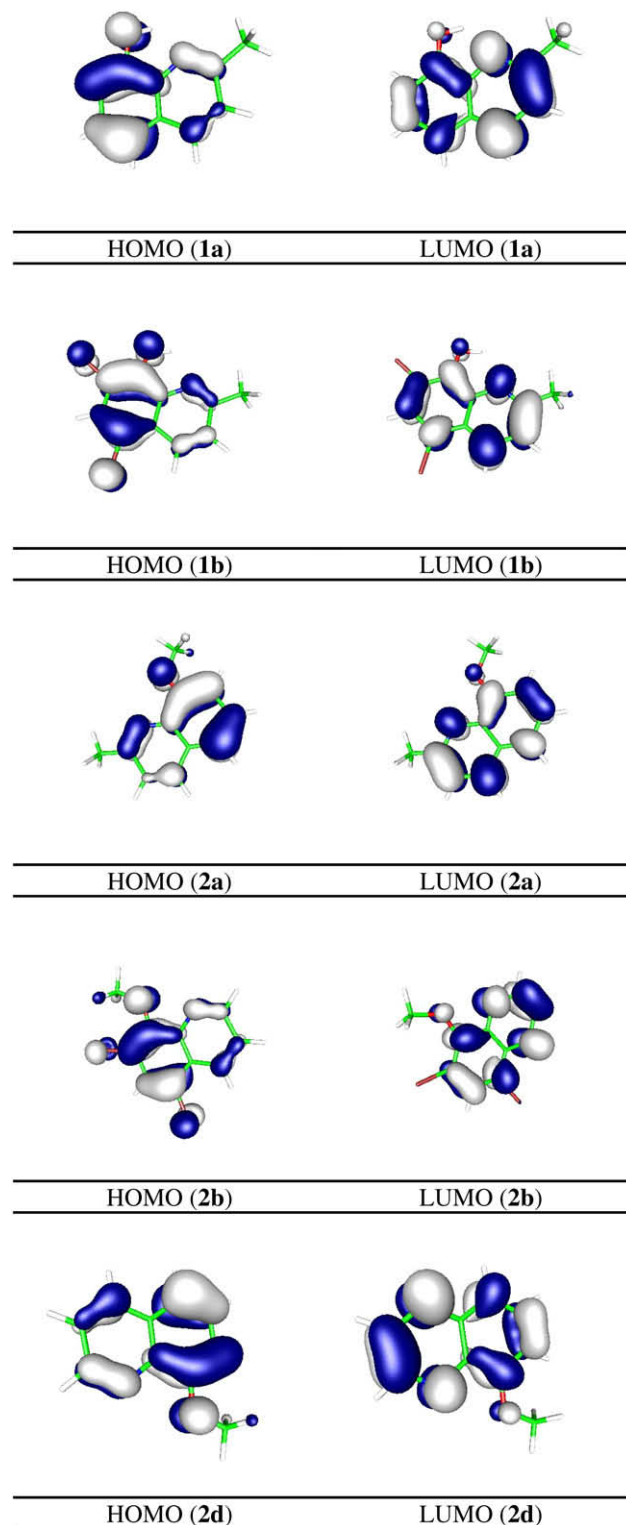


Fig. 6. Contours of HOMO and LUMO orbitals of studied compounds.

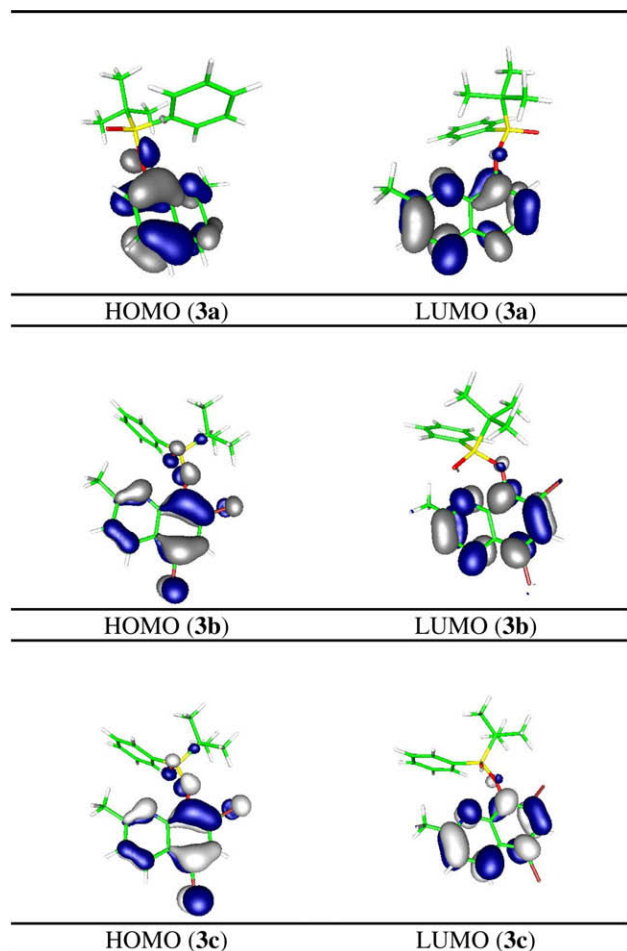


Fig. 6 (continued)

donating and accepting sites between the pyridine and hydroxylic functions, mimicking previously described behaviors of some hydroxyquinoline carboxylic acids [10]. Compound **1a** crystallises in space group *Pbca* (no. 61), compound **1b**, in *C1 2/c 1* (no. 15). The molecular ring systems are both essentially planar. The molecules of **1a** are linked by weak bifurcated O1–H1A...N2A, O1–H1A...N1 and O2AH1BA...N2A, O2AH1BA...N1 hydrogen bonds. For **1b** it is through strong O1–H1A...N1A and O1A–H1AA...N1 hydrogen bonds.

Compound **2a** crystallises in space group *C1 2/c 1* (no. 15). The molecular ring system is essentially planar (see Fig. 3 and Table 3).

The detailed study of peaks on the difference Fourier map showed that in the position of one of the **2a** molecule, there is one molecule of 2-methylquinolin-8-ol (**1a**). The lack of the additional reflections from superstructure is evidence that these molecules are disordered. The refinement showed that the occupancy of **1a** is equal to 0.078(2), which caused the decrease of R1 value from 5.59% to 3.04% and the maximum on the difference Fourier map from 1.03 eÅ⁻³ to 0.20 eÅ⁻³. In spite of this, such attempts do not change the molecular parameters. The high quality crystals of **2a** grew only from the crude product (see Figs. 4 and 5).

Compounds **3a** and **3b** crystallized in space group *P121/c1* (no. 14), and their molecular ring systems (quinoline) are essentially planar. In both cases the molecules are linked by weak C–H...O hydrogen bonds (Tables 4 and 5).

The development of new and more efficient methodologies to transform hydroxyhaloquinolines to their derivatives which could help to look deeper into reasons of HIV inhibition is a subject of continuous interest in our laboratory [10,13–18]. To understand

their reactivity we compared selected geometric parameters such as bond lengths and bond angles presented on Tables 1–5.

Comparing the structural parameters of hydroxyhaloquinolines **1a** and **1b** with the data of their derivatives, such as ether **2a**, esters **3a** and **3b** shows significant differences. Esters possess much longer C7–O1 bond lengths because of the electron withdrawing ability of P=O group. For the same reason the P=O group could induce shortened C4–C11 and C6–C12 bonds. Meanwhile, the existence of halogen atoms could cause an abridgement of C7–O1 bond. We also observed the electronic influence of oxygen from C7–O1 on both bond lengths C4–C11 and C6–C12 of compounds **1b** and **3b** (see Table 6).

3.1. NMR

Recently we studied ¹³C and ¹⁵N NMR spectra demonstrating proton transfer reactions between the pyridine and carboxylic acid functions of some hydroxyquinoline carboxylic acids [10]. The ¹H and ¹³C NMR spectra of **1a–c**, **2a,b** and **3a–c** displayed readily diagnostic signals from methyl protons and carbon atoms. Analysis of the trend in ¹H chemical shifts revealed that the presence of P=O, compared to the methyl of ether or H of hydroxylic group, significantly increased the deshielding effects on proton. Similar effect in ¹³C chemical shifts was observed. Halogen (Cl or Br) atoms at 5 and 7 positions have weaker effects on the ¹H and ¹³C chemical shifts of methyl group.

3.2. IR

In the studied compounds the bands of C=C and C=N stretching modes were observed at 1600, 1608, 1603, 1605, 1617, 1604, 1596, 1585 cm⁻¹ for **1a**, **1b**, **2a**, **2b**, **2d**, **3a**, **3b** and **3c**, respectively. The ν_{O–H} had the maxima at 3278 cm⁻¹ (**1a**) and 3274 cm⁻¹ (**1b**), respectively. The bands at 1263 and 1031 cm⁻¹ indicated the ether group in the compound **2a**. Strong band corresponding to the stretching vibration of P=O group in **3a** and **3b** appeared at 1229 and 1244 cm⁻¹, respectively. The maxima at 2960, 2939, 2946 and 3066 cm⁻¹ are related to stretching modes of *tert*-butyl and methyl fragments in studied compounds. More details of the vibrational spectra of the compounds are given in the Table S1.

3.3. DFT calculations

The calculations were carried out using Gaussian03 [19] program. The DFT/B3LYP [20,21] method was used for the geometry optimization and electronic structure determination. Electronic spectra were calculated by TDDFT [22] method. The calculations were performed with polarization functions for all atoms: 6-31g(2d,p) – chlorine, bromine and phosphorus, 6-31g** – carbon, nitrogen and 6-31g(d,p) – hydrogen. The PCM solvent model was used in the Gaussian calculations with dichloromethane as the solvent. The contribution of molecular orbitals in the electronic transitions was calculated using Gausssum software [23].

3.4. Optimized geometries

The geometries of the studied compounds were optimized in singlet states using the DFT method with the B3LYP functional. In general, the predicted bond lengths and angles are in a good agreement with the values based on the X-ray crystal structure data. The general trends observed in the experimental data were well reproduced in the calculations.

The maximum differences between optimized and experimental geometry of the heteroatoms and carbons in studied compounds are visible in distances: O(1)–C(7) 0.008 Å, O(1)–C(7) 0.017 Å, Cl(1)–C(5) 0.011 Å, P(1)–O(1) 0.048 Å and P(1)–O(1)

0.053 Å in compound **1a**, **1b**, **2a**, **3a** and **3b**, respectively. In the angles differences do not outrun 2°.

Although the X-ray structures of the compounds **2b**, **2d** and **3c** were not determined, their geometries, IR frequencies and electronic transitions were calculated. A good agreement of the calculated spectroscopic properties of **2b**, **2d** and **3c** with the experimental ones (Fig. S1) indicates that the calculated geometries correspond well to the real structures. The maximum error between the calculated and experimental IR frequencies is about 4.3%, 8.2% for **2b**, **2d** and 7.8% for **3c**.

3.5. Electronic structure and NBO analysis

The HOMO and LUMO orbitals of studied compounds are presented in Fig. 6. The HOMO orbitals of the studied compounds are composed from π_C and π_O hydroxyquinoline moiety and in LUMO π nitrogen orbitals played a role. The heteroatoms of studied compounds contributed in the low molecular orbitals. The HOMO-6 of **3a** is composed of $\pi_{O(P)}$ (56%) and $\pi_{O(quinoline)}$ (18%). HOMO-9 of **3b** is localized mainly on the chlorines. On the phosphinate moiety,

the localized molecular orbitals are from HOMO-3, 4, 5 in compound **3a**, and are from HOMO-2 and HOMO-4 in **3b**. The virtual MO LUMO + 2, LUMO + 4 in **3a** and LUMO + 2 and LUMO + 3 in **3b** are composed from phosphinate. The eigenvalues of the HOMO and LUMO molecular orbitals in studied compound are negative (**1a** – HOMO –5.70; LUMO –1.32; **1b** – HOMO –5.56; LUMO –1.01; **2a** – HOMO –5.98; LUMO –1.67; **2b** – HOMO –5.91; LUMO –1.63; **2d** – HOMO –5.65; LUMO –1.14; **3a** – HOMO –6.06; LUMO –1.34; **3b** – –6.23; LUMO –1.71; **3c** – HOMO –6.12; LUMO –1.69 eV). Nevertheless, the electron acceptor ability of the LUMO may play a greater role than the electron donation of the HOMO. The LUMO eigenvalues are far less negative compared to the HOMO eigenvalues whatever indicating a strong affinity for electrons.

Basing on the NBO theory [24] the stabilization energy [25] were calculated and shown that the molecules were stabilised by the donation of charge from N-C to antibonding orbital of C-C (for example $\Delta E_{ij} = 120.39$ (**1a**); 261.32 (**1b**); 168.37 (**2b**) kcal/mol). In the molecules **2a**, **3a** and **3b** the stabilisation is visible in the donation of hydroxyquinoline oxygen to the antibonding orbital of C-C and phosphorus empty d orbitals.

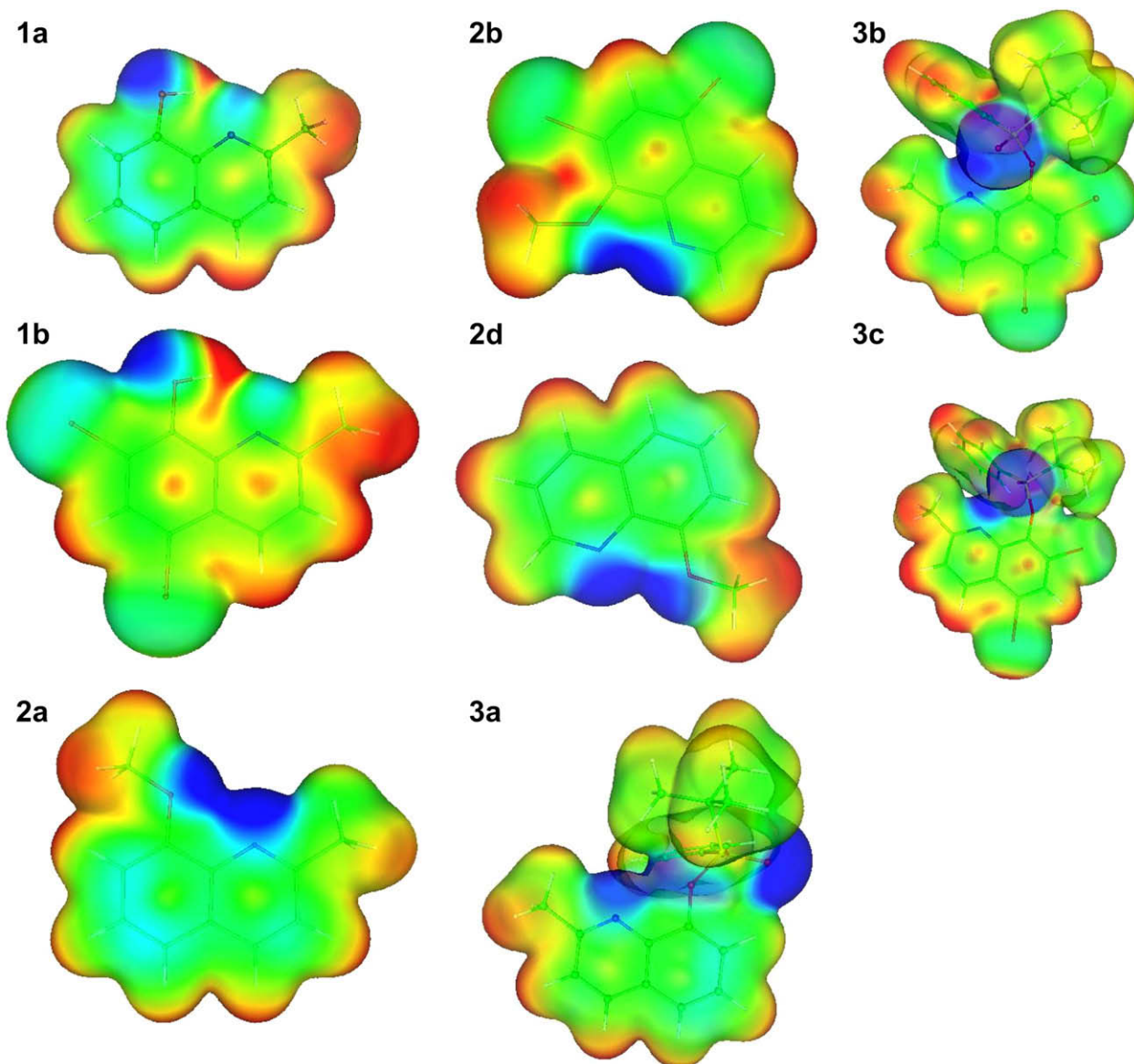


Fig. 7. Electrostatic potential densities of the compounds **1a**, **1b**, **2a**, **2d**, **3a** and **3b** at the electron density of 0.005 a.u.

The heteroatoms charges of the studied compounds taking from Natural Population Analysis are as follow: **1a**: N –0.509, O –0.691; **1b**: N –0.444, O –0.501; **2a**: N –0.501, O –0.672, Cl –0.004, 0.023; **2b**: N –0.426, O –0.501, Cl –0.004; **2d**: N –0.430, O –0.499; **3a**: P 2.256, O_{hydroxyqu} –0.808, O_{phosphorus} –1.086, N –0.467; **3b**: Cl 0.001, 0.020, P 2.257, O_{hydroxyqu} –0.808, O_{phosphorus} –1.067, N –0.455; **3c**: Br 0.066, 0.089, P 2.257, O_{hydroxyqu} –0.807, O_{phosphorus} –1.066, N –0.453. In this study the chlorine and bromine substituents for **1b**, **2b**, **3b** and **3c** are almost neutral, which could explained the difficulties with the preparation of arylphosphanes using halogenoaryls [18]. The charges on the quinoline nitrogen atom increased in compounds, and the charge on the quinoline oxygen declined. The atomic charge calculations can be indicative for the relocation of the electron density of the compounds, but the local concentration and local depletion of electron charge density allow us to determine whether the nucleophile or electrophile can be attracted. Because the electron distribution is not apparent from the partial atomic charges in Fig. 7, it only gives the plots of the electrostatic potentials for the studied compounds. The isoelectronic contours are plotted at 0.005 a.u. (3.1 kcal/mol). The color code of these maps is in the range of 0.005 a.u. (deepest red) to –0.005 a.u. (deepest blue) in all compounds, where blue indicates the strongest attraction and red indicates the strongest repulsion. Regions of negative $V(r)$ are usually associated with the lone pair of electronegative atoms. The negative potential in the studied compounds wraps the nitrogen, oxygen and phosphorus atoms.

3.6. Electronic spectra

Experimental electronic spectra measured in dichloromethane solutions along with the theoretical electronic absorption spectra calculated on the B3LYP/6–31G* level optimized structures are listed in Table 7. The calculations of electronic spectra were performed using PCM model. The experimental spectra are presented

Table 7
Experimental and theoretical electronic absorption spectra values for studied compounds.

Experimental	Calculated	Oscillator strength	Most important configurations
1a			
306.0	325.8	0.043	H → L (87%)
	279.5	0.010	H-1 → L (42%), H → L + 1 (57%)
1b			
318.0	307.4	0.076	H → L (86%)
2a			
300.0	327.0	0.065	H → L (86%)
	292.0	0.008	H-1 → L (38%), H → L + 1 (62%)
2b			
326.4	326.7	0.103	H → L (86%)
300.8	289.5	0.011	H-1 → L (35%), H → L + 1 (65%)
	285.5	0.002	H-2 → L (94%)
2d			
303.2	313.2	0.082	H → L (86%)
	278.3	0.004	H-1 → L (40%), H → L + 1 (60%)
	278.1	0.003	H-2 → L (94%)
3a			
319.3	294.7	0.098	H → L (84%)
283.4	279.9	0.013	H-2 → L (87%), H → L + 1 (23%)
272.9	267.7	0.021	H → L + 1 (72%), H → L + 2 (19%)
3b			
300.2	307.0	0.160	H → L (84%)
	292.9	0.010	H-5 → L (14%), H-1 → L (72%)
3c			
301.8	311.6	0.173	H → L (84%)
	293.9	0.001	H-5 → L (15%), H-1 → L (73%)
	290.1	0.006	H-2 → L (52%), H → L + 1 (49%)

in Figs. S2–S4. Electronic absorption spectra display bands with the maximums at **1a** – 306.0 nm, **1b** – 318.0 nm, **2a** – 300.0 nm, **2b** – 326.4, 300.8 nm, **2d** – 303.2 nm, **3a** – 319.3, 283.4, 272.9 nm and **3b** – 300.2 nm, **3c** – 301.8 nm. The first calculated transitions in the studied compounds were derived from HOMO → LUMO excitation (**1a** – 87%, **1b**, **2a–c** – 86%, **3a,b** – 84%, **3c** – 85%).

Shoulders on the spectra of compound **3a**, **3b** and **3c** are associated with the transitions in which heteroatoms (P, O, N) π orbitals play significant roles. Molecular orbital coefficients analyses based on the optimized geometry indicate that the frontier molecular orbitals are mainly composed of p atomic orbitals, so electronic transitions corresponding to above electronic spectra are mainly assigned to $n \rightarrow \pi^*$ and $\pi \rightarrow \pi^*$ electronic transitions.

4. Conclusion

In the present studies, we report the synthesis and characterization of some methyl and phosphinyl derivatives of 2-methylquinolin-8-ol (**1a**) and related 5,7-dichloro-2-methylquinolin-8-ol (**1b**) using microanalyses (C,H,N), IR, UV–vis, multinuclear NMR spectroscopic techniques. Five of them have been characterized by single crystal X-ray diffraction method.

X-ray crystal structure analysis of **1a** and **1b** showed the presence of hydrogen-bond donating and accepting sites between the pyridine and hydroxylic functions.

The ^1H and ^{13}C NMR spectra of **1a–c**, **2a,b** and **3a–c** displayed readily diagnostic signals from methyl protons and carbon atoms. Analysis of the trend in ^1H chemical shifts revealed that the presence of P=O, compared to the methyl of ether or H of hydroxylic group, significantly increased the deshielding effects on proton. Halogen (Cl or Br) atoms at 5 and 7 positions have weaker effects on the ^1H and ^{13}C chemical shifts of methyl group.

The NBO studies showed us that the chlorine and bromine substituents for **1b**, **2b**, **3b** and **3c** are almost neutral. The charges on the quinoline nitrogen atom increased in compounds, and the charge on the quinoline oxygen declined. The atomic charge calculations are the indication of the relocation of the electron density of the compounds, but the local concentration and local depletion of electron charge density allow us to determine whether the nucleophile or electrophile can be attracted.

Acknowledgments

We thank Professor Dietrich Gudat for NMR spectra and the ICN Polfa Rzeszow S.A. for a sample of 5,7-dichloro-2-methylquinolin-8-ol.

Appendix A. Supplementary data

Supplementary data associated with this article can be found, in the online version, at doi:10.1016/j.molstruc.2010.01.054.

References

- [1] D. De, L.D. Byers, D.J. Krogstad, J. Heterocycl. Chem. 34 (1997) 315.
- [2] P.M. O'Neill, P.G. Bray, S.R. Hawley, S.A. Ward, B.K. Park, Pharmacol. Ther. 77 (1998) 29.
- [3] J.N. Dominguez, Curr. Top. Med. Chem. 2 (2002) 1173.
- [4] P.B. Madri, J. Sherrill, A.P. Liou, J.L. Weisman, J.L. DeRisi, R.K. Guy, Bioorg. Med. Chem. Lett. 15 (2005) 1015–1018.
- [5] J.N. Delgado, A.W. Remers, in: J.N. Delgado, A.W. Remers, (Eds.), Wilson and Gisvold's Textbook of Organic Medicinal and Pharmaceutical Chemistry, 9th ed., J.B. Lippincott Company, Philadelphia, 1991.
- [6] P.M. O'Neill, P.G. Bray, S.R. Hawley, S.A. Ward, B.K. Park, Pharmacol. Ther. 77 (1998) 29–58.
- [7] G. Blauer, M. Akkawi, W. Fleischhacker, R. Hiessböck, Chirality 10 (1998) 556–563.
- [8] T.J. Egan, R. Hunter, C.H. Kaschula, H.M. Marques, A. Mispion, J. Walden, J. Med. Chem. 43 (2000) 283–291.

- [9] F. Zouhiri, J.F. Mouscadet, K. Mekouar, D. Desmaele, D. Savoure, H. Leh, F. Subra, M.L. Bret, C. Auclair, J. d'Angelo, *J. Med. Chem.* 43 (2000) 1533–1540.
- [10] D. Gudat, J.E. Nycz, J. Polanski, *Magn. Reson. Chem.* 46 (2008) 115–119.
- [11] G.M. Sheldrick, *Acta Cryst. A* 64 (2008) 112–122.
- [12] G.M. Sheldrick, SHELXS97 and SHELXL97, University of Göttingen, Germany, 1997.
- [13] J. Chojnacki, P. Skop, A. Pladzyk, J.E. Nycz, *Acta Cryst. E* 63 (2007) o4773–o4774.
- [14] L. Ponikiewski, J.E. Nycz, *Acta Cryst. E* 65 (2009) o515–o530.
- [15] B. Machura, J. Miłek, J. Kusz, J. Nycz, *D. Tabak, Polyhedron* 27 (2008) 1121–1130.
- [16] J.E. Nycz, *Polish J.Chem.* 83 (2009) 589–594.
- [17] J.E. Nycz, *Polish J.Chem.* 83 (2009) 1637–1642.
- [18] J.E. Nycz, *Phosphorus Sulfur Silicon Relat. Elem.* 184 (2009) 2605–2612.
- [19] M.J. Frisch, G.W. Trucks, H.B. Schlegel, G.E. Scuseria, M.A. Robb, J.R. Cheeseman, J.A. Montgomery, Jr., T. Vreven, K.N. Kudin, J.C. Burant, J.M. Millam, S.S. Iyengar, J. Tomasi, V. Barone, B. Mennucci, M. Cossi, G. Scalmani, N. Rega, G.A. Petersson, H. Nakatsuji, M. Hada, M. Ehara, K. Toyota, R. Fukuda, J. Hasegawa, M. Ishida, T. Nakajima, Y. Honda, O. Kitao, H. Nakai, M. Klene, X. Li, J.E. Knox, H.P. Hratchian, J.B. Cross, C. Adamo, J. Jaramillo, R. Gomperts, R.E. Stratmann, O. Yazyev, A.J. Austin, R. Cammi, C. Pomelli, J.W. Ochterski, P.Y. Ayala, K. Morokuma, G.A. Voth, P. Salvador, J.J. Dannenberg, V.G. Zakrzewski, S. Dapprich, A.D. Daniels, M.C. Strain, O. Farkas, D.K. Malick, A.D. Rabuck, K. Raghavachari, J.B. Foresman, J.V. Ortiz, Q. Cui, A.G. Baboul, S. Clifford, J. Cioslowski, B.B. Stefanov, G. Liu, A. Liashenko, P. Piskorz, I. Komaromi, R.L. Martin, D.J. Fox, T. Keith, M.A. Al-Laham, C.Y. Peng, A. Nanayakkara, M. Challacombe, P.M.W. Gill, B. Johnson, W. Chen, M.W. Wong, C. Gonzalez, J.A. Pople, *Gaussian 03, Revision B.03*, Gaussian, Inc., Pittsburgh PA, 2003.
- [20] A.D. Becke, *J. Chem. Phys.* 98 (1993) 5648–5652.
- [21] C. Lee, W. Yang, R.G. Parr, *Phys. Rev. B* 37 (1988) 785–789.
- [22] M.E. Casida, in: J.M. Seminario (Ed.), *Recent Developments and Applications of Modern Density Functional Theory, Theoretical and Computational Chemistry*, vol. 4, Elsevier, Amsterdam, 1996, p. 391.
- [23] N.M. O'boyle, A.L. Tenderholt, K.M. Langner, *J. Comp. Chem.* 29 (2008) 839–845.
- [24] P. Foster, F. Weinhold, *J. Am. Chem. Soc.* 102 (1980) 7211–7218; K. Eichkorn, F. Weigend, O. Treutler, R. Ahlrichs, *Theor. Chim. Acc.* 97 (1997) 119–124.
- [25] Peter Müller (Ed.), *Crystal Structure Refinement: A Crystallographer's Guide to SHELXL*, IUCr/Oxford, 2006.